ACS APPLIED MATERIALS & INTERFACES

www.acsami.org
Research Article

Charge Injection and Interfiber Electrical Conduction in Cable Bacteria

Cosimo Tommasi,* Anastasia Gerzhik, Sebastian Heinzmann, Silvia Hidalgo Martinez, Dirk Mayer, Filip. J. R. Meysman, and Herre S. J. van der Zant*

Cite This: ACS Appl. Mater. Interfaces 2026, 18, 25038−25043
Read Online

ABSTRACT: Cable bacteria are multicellular microorganisms capable of charge transport over centimeter-scale distances through a network of conductive fibers embedded in the cell envelope. Understanding the charge injection mechanism into these fibers is essential to obtain a complete picture of their long-distance charge transport and a crucial step for their application in biobased electronics. To this aim, we fabricated "crosses" of two filaments, either native bacteria or extracted fiber skeletons, placed one on top of each other. By probing charge transport both through individual filaments and in cross-cable configurations, i.e., with current flowing from one filament to the other, it is possible to isolate the charge injection contribution. The results indicate that charge transfer between two contacting fibers is possible, albeit with increased resistance. We characterized the crosses at different temperatures, from 300 down to 50 K, observing thermally activated Arrhenius behavior both for single filaments and cross-conduction. The corresponding activation energy for filament-to-filament transport ranged from 15 to 40 meV, slightly smaller than that of individual cable bacterium filaments. We conclude that charge injection into the fibers must rely on the same mechanism as charge transport along the fibers. A structural model of the fibers is proposed in which internally winding conductive channels are embedded in a protein matrix. These channels can locally reach the surface of the fibers, where they can establish electrical contact with the external environment.

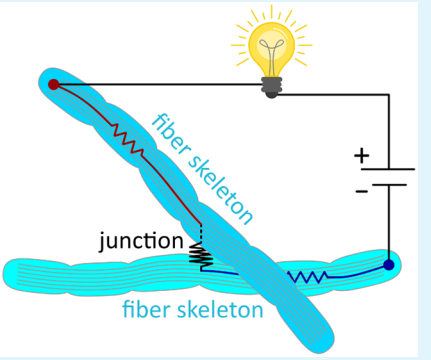

KEYWORDS: *cable bacteria, biological conduction, charge injection, temperature dependence, inter-fiber transport*

INTRODUCTION

Cable bacteria are multicellular organisms that form a linear chain of cells through which electrical currents run over centimeter-scale distances. Relaying electrons from one end to the other is essential for their metabolism, and the capability of long-range transport equips them with a competitive advantage for harvesting electron donors in aquatic sediments.[1,2] While there are many examples of charge transport in biological systems, cable bacteria stand out for two remarkable properties. First, the length scale over which they conduct electrical currents is orders of magnitude larger than any other biological system. While electron transport is known to range from nanometers in the electron transport chain of chloroplasts and mitochondria,[3−5] up to micrometers in bacterial appendages[6,7] it extends up to a few centimeters in cable bacteria.[8,9] Second, the reported conductivity values for the conductive structures inside cable bacteria are as high[9−12] as 500 S cm^{-1}. This extraordinary conductivity exceeds that of other biological conductors by orders of magnitude and even outclasses the conductivity of most highly doped organic semiconductors.[13] Such characteristics set cable bacteria aside from other biobased conductors, and recent studies indicate that the mechanism governing the electrical transport might also be different from conductive conventional protein systems that incorporate hemes or FeS clusters as cofactors.[9,11,12,14,15]

The discovery of highly efficient conduction in cable bacteria has attracted attention from a range of disciplines. On one hand, long-range electron transport exerts an important influence on the functioning of natural ecosystems, while on the other hand the prospect of a biobased material with exceptional electrical properties has intriguing applications in the field of material science. Until present, scientific attention has been primarily focused on the elucidation of the conductive structure inside cable bacterium filaments.[9,14,16−18] To mediate electrical currents, cable bacteria, such as *Ca.* Electrothrix gigas, contain an internal network of ≈60 fibers (≈50 nm diameter each) that are positioned in parallel within the shared periplasm of the multicellular filaments.[19,20] Recent investigations reveal that each fiber contains ≈15 thinner strands, twisting together and embedded into an organic

Received: January 23, 2026
Revised: April 8, 2026
Accepted: April 9, 2026
Published: April 22, 2026

protein matrix.[14,17,18] The strands themselves provide a highly efficient one-dimensional channel for long-distance electron transport, and spectroscopy studies show that they contain a conjugated nickel bis(1,2-dithiolene) structure.[16,18] While these studies greatly extended our understanding of the conductive structures in cable bacteria, a detailed structural model is still missing. Mass spectroscopy data suggests that the conductive channels are sheathed by an insulating protein layer, forming a core−shell structure.[14,21] The model above describes how electrons are transported along the filaments, but poses questions about how charge can be injected and extracted from the fiber network. In fact, while the contact resistance to fiber skeletons has already been addressed in the literature[9,12] the mechanism by which charges can tunnel through the insulating protein shell is still elusive.

Insight into charge injection would not only be relevant for the biology of electron uptake in cable bacteria, but will also play a key role in the future development of bioelectronic devices. Indeed, the conductive fibers in cable bacteria are proposed to be a promising candidate material for the development of functional biobased electronics.[9,17] Such devices would be composed of meshed, interconnected wires: charge injection from a wire into another will play a fundamental role in determining the overall electrical properties of the material. Here, we examine how charge can be injected into fibers and probe the possibility of "inter-fiber" transport. To this end, we realize contact between fibers of two different filaments, placing one on top of the other. By connecting to each end of both filaments we probe both single-cable and cross-cable conduction, and monitor it from room temperature down to ≈50 K. We compare results for devices realized from native cable bacteria, and from extracted fiber skeletons.

MATERIALS AND METHODS

Electrical characterization was performed on samples composed by two conductive filaments placed one on top of each other, forming an "X" configuration (Figure 2). The filaments are native cable bacteria or fiber skeletons obtained by sequential extraction of native cable bacteria (all derived from a clonal culture of *Candidatus* Electrothrix gigas). The extraction procedure removes membranes and cytoplasm, but retains the conductive fibers embedded in a sheath (i.e., the fiber skeleton); see SI for additional details on the extraction procedure. A fiber skeleton (thickness 150−200 nm) is considerably thinner than a native filament (thickness 1000−3000 nm), but the fibers retain their original diameter ≈50 nm; moreover, previous work has shown that the extraction process does not affect the fiber conductivity.[9] A scanning electron microscope image of a fiber skeleton is shown in Figure 1.

For each sample, two filaments of the same type were manually deposited onto an insulating substrate (glass coverslips or silicon chips capped with 1 μm silicon oxide). While we aimed for a perpendicular crossing, the contact angle was not always 90 degrees due to the difficulty of positioning the filaments. Possible implications of this variation in contact angle are discussed later in the text. The terminal ends of the filaments were electrically contacted by establishing ad hoc contacts with carbon paint (EM-Tec C30) or by carefully aligning the filaments onto prepatterned gold electrodes (Figure 2a). In both cases, the distance between opposite contacts was ≈1 mm. Since conductivity of cable bacteria is known to degrade when exposed to oxygen[9,22] extreme care was used when handling the filaments. Filament picking and extraction was performed in an anoxic glovebox environment, and samples were transported in a commercial vacuum container. A total of 7 different samples were realized and tested (5 fiber skeletons, 2 native cable bacteria). Further details about sample fabrication and characteristics can be found in the SI.

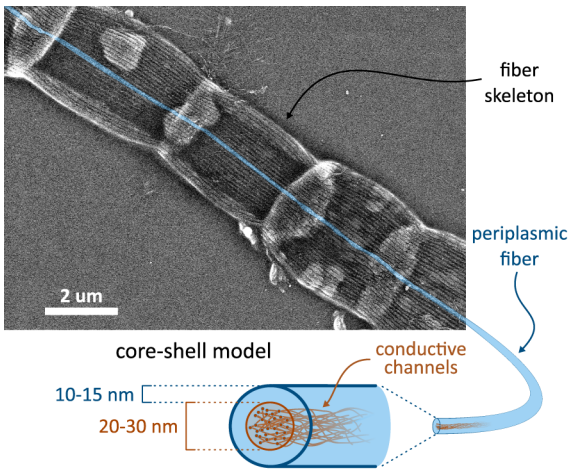

Figure 1. Scanning electron microscope image of an extracted fiber skeleton, showing multiple cells. Each cell is about 2 × 3 μm^2, with the cell interfaces appearing as brighter areas. The top ridges corresponding to the conductive periplasmic fibers are visible; one of them is highlighted in blue for clarity. The schematic on the bottom shows its internal structure according to the core−shell model. The core and shell dimensions are those reported in.[14,21]

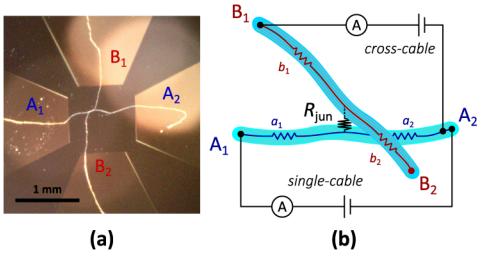

Figure 2. (a) optical microscope picture of a fiber skeleton "cross", with four gold pads contacting one end of a filament each. The distance between opposite gold electrodes is 1 mm. (b) equivalent circuit of the skeleton "cross", with each cable split in a series of two resistances, $a_1 + a_2$ and $b_1 + b_2$ respectively. Where the cables overlap, they are connected by a junction resistance R_{jun}. The two measurement configurations are depicted, either connecting two ends of the same filament (*single-cable*) or two ends of different filaments (*cross-cable*). The ends of the skeletons are labeled [A_1, A_2] and [B_1, B_2] respectively.

We probed our devices using a CRX-6.5K cryogenic probe station (Lakeshore cryotronics) connected to a homemade electronics rack and a multimeter (Keithley DMM6500). We performed two-probe electrical characterization, acquiring current−voltage ($I-V$) curves at different temperatures. Measurements were always performed in vacuum (≈10^{-6} mbar), while the temperature was varied from room temperature down to ≈50 K. The lower bound for the measured temperatures was determined by the behavior of the $I-V$ curves: below 50 K the RC time of the measured circuit becomes very large, and the $I-V$ hence show marked hysteresis, thus precluding the extraction of the sample's resistance from the $I-V$ curves. We therefore limit ourselves to the temperature range where all $I-V$ curves do not exhibit noticeable hysteresis.

Each device has four contacts. By connecting two at a time, it is possible to realize six different configurations (see schematic in Figure 2b). In the "single-cable" configurations, both contacts belong to the same filament, and the current flows solely through that filament ($A_1 - A_2$ in Figure 2b). In a "cross-cable" configuration, the terminal ends of different filaments are connected ($B_1 - A_2$ in Figure 2b), and so, current must flow from one filament to the other. In the following, we refer to the interfilament contact (center of the X) as "junction".

https://doi.org/10.1021/acsami.6c01506
ACS Appl. Mater. Interfaces 2026, 18, 25038−25043

For each device, $I-V$ curves were recorded for all possible single-cable and cross-cable configurations. From each $I-V$ curve we extracted the low-bias resistance R by fitting a linear least-squares model to the data at $|V| < 150$ mV. In this bias window, the $I-V$ traces were linear and contained at least 9 data points, thus providing sufficient data for linear fitting. We label the resistances with their contact codes, e.g., $R_{A_1A_2}$ for a single-cable configuration and $R_{A_1B_1}$ for a cross-cable configuration.

Calculation of the Junction Resistance

Assuming additive behavior of the resistances, it is possible to schematize the crosses as a system of five resistances. The resistance of each filament is split into two components (representing the segment before and after the junction; Figure 2b):

$$R_{A_1A_2} = a_1 + a_2$$
$$R_{B_1B_2} = b_1 + b_2 \quad (1)$$

The junction itself is modeled as a simple resistance R_{jun} connecting the two wires. The different resistances measured in the cross-cable configurations can be then expressed in terms of a_i, b_i components (i = 1, 2) and junction resistance:

$$\begin{cases} R_{A_1B_1} = a_1 + R_{jun} + b_1 \\ R_{A_2B_2} = a_2 + R_{jun} + b_2 \\ R_{B_1A_2} = b_1 + R_{jun} + a_2 \\ R_{B_2A_1} = b_2 + R_{jun} + a_1 \end{cases} \quad (2)$$

By suitable summation of expressions in eq 2 and substitution of eq 1, we get two expressions for R_{jun} that are solely based on measured quantities:

$$R_{jun,1} = \frac{1}{2}(R_{A_1B_1} + R_{A_2B_2} - R_{A_1A_2} - R_{B_1B_2})$$
$$R_{jun,2} = \frac{1}{2}(R_{B_1A_2} + R_{B_2A_1} - R_{A_1A_2} - R_{B_1B_2}) \quad (3)$$

While theoretically, these expressions should yield the same value for R_{jun}, they typically slightly differ when calculated starting from experimental quantities. In the following we employ the average value to eventually arrive at the zero-bias conductance:

$$G_{jun} = \left(\frac{R_{jun,1} + R_{jun,2}}{2}\right)^{-1} \quad (4)$$

RESULTS AND DISCUSSION

Cross-Cable Conduction Occurs in Fiber Skeletons

Room-temperature characterization of cross-devices with native filaments revealed a current flow in the single-cable configuration, but not in the cross-cable configuration (Figure 3a). Native cable bacteria filaments showed a highly linear $I-V$ curve, consistent with previous observations.[9,10,12] The corresponding low-bias resistances were in the MΩ range (Table S1 in the SI), matching expectations for millimeter-length conduction along native cable bacteria filaments.[8,10] The cross-cable configurations behaved like an open circuit (Figure 3a), with currents remaining below current detection level (<1 pA). We ascribe this lack of conduction across the junction to the presence of cell material (outer cell membranes, periplasmic protein), which apparently forms a too high resistive barrier between the conductive fiber networks that are more deeply embedded in the filaments. We remark that the same cellular membrane is present also where the native filaments make contact with the electrodes.

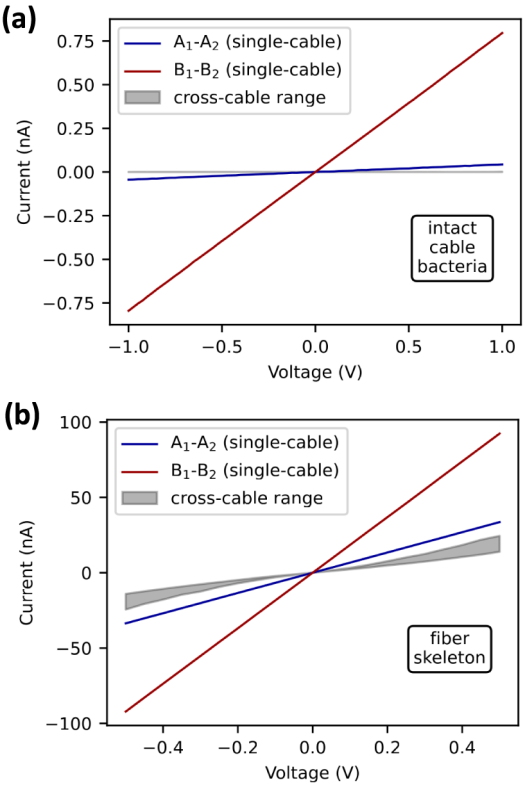

Figure 3. Current–voltage ($I-V$) curves of the two single-cable configurations (A_1-A_2 and B_1-B_2, solid lines) and of all the cross-cable configurations (shaded region) for: (a) a native cable bacteria cross and (b) a fiber skeleton cross. Four different cross-cable configurations can be realized, and all their $I-V$ curves fall into the shaded region. Native cable bacteria do not show cross-cable conduction. All $I-V$ curves are acquired at room temperature and in vacuum. See Table S1 in the SI for details of the samples.

Room-temperature measurements of cross-devices with fiber skeletons revealed a current flow in both single-cable and cross-cable configurations (Figure 3b). Individual fiber skeletons exhibited linear $I-V$ curves, as seen for native filaments, but yielded lower resistances compared to them (Table S1). The cross-cable configuration revealed that interfilament conduction across the junction is possible (Figure 3b). Apparently, the fiber skeleton extraction procedure removes enough cell material so that the conductive fiber networks of different filaments become electrically connected. The currents measured in the four different cross-cable configurations of a single device are smaller than the single-cable configurations. Notably, these four $I-V$ curves are all very similar (shaded region in Figure 3b) and markedly nonlinear (see also Figures S1–S2). This indicates that the junction between the two filaments acts as a barrier for charge transport and represents the bottleneck for conduction in the cross-cable configuration, therefore R_{jun} dominates the overall resistance. This in turn implies that the individual filament segments have negligible influence on the $I-V$ characteristics of cross-cable configurations, and so the junction resistance becomes independent of the filament segment lengths. Additionally, we highlight that when calculating the junction resistance from eq 3 the contributions from the 4 individual filament segments cancel out. The same behavior was consistently observed in other 4 replicate devices with junction resistances spanning several orders of magnitude (see Table S1

https://doi.org/10.1021/acsami.6c01506
ACS Appl. Mater. Interfaces 2026, 18, 25038–25043

in the SI). Some degree of variability is to be expected, since the junction area is influenced by the contact angle of the two filaments, and the junction resistance is expected to be inversely proportional to its area. While we did not measure such area, nor the angle between the filaments, we can still estimate the magnitude of such geometric effect. Assuming a manual error in the placement of the fibers of 60 degrees, the area increases by just a factor 2. We thus ascribe the much larger observed variability to some other effect at the interface that might become clearer once the conduction mechanism at the junction has been explained.

Cross-Cable Junctions Show Similar Activation Energy as the Single Cables

Conductance in cable bacteria is known to follow an Arrhenius behavior $G(T) \propto \exp(-E_a/k_B T)$ over the temperature range from 100 to 300 K, with an activation energy E_a of about 50 meV.[10,12] While the microscopic origin of such activation energy has not been clarified yet, its low value (when compared to other examples of biological transport) is characteristic of *Candidatus* Electrothrix gigas, and is closely related to the molecular structures enabling charge transport in their fibers.[10,12,15] Measurements on fiber skeletons (Figure 4)

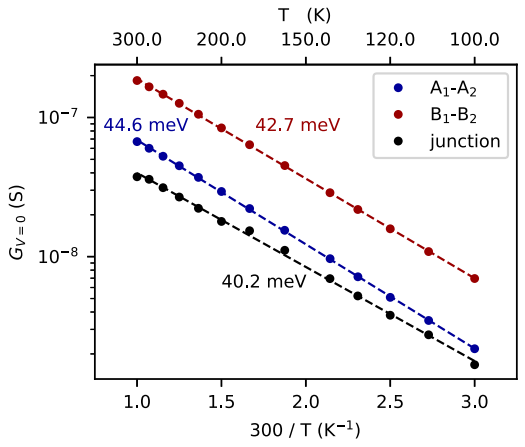

Figure 4. Zero-bias conductance vs inverse temperature (300−100 K) for the two single-cable configurations, and for the junction conductance as obtained from eq 4. Dashed lines indicate the Arrhenius fits to the data; the corresponding activation energies are shown with the same color.

and native cable bacteria (Figure S11) in the single-cable configuration confirm this behavior. By also measuring cross-cable configurations and using eqs 3 and 4, we were able to isolate the temperature dependence of the junction resistance (black data set in Figure 4). Remarkably, R_{jun} also showed Arrhenius behavior, although with a slightly lower activation energy than the individual filaments. Other cross-devices of fiber skeletons showed similar results, with even smaller activation energies (15−24 meV, Table S1).

Biological electron transport is commonly described by the classical Marcus theory of nonadiabatic electron hopping.[12,23] In this framework, one of the key parameters governing transport is the reorganization energy λ, which is approximated as $\lambda \simeq 4E_a$. This quantity can be interpreted as the energy required to reorganize the dielectric environment of the charge carrier site and its surroundings, when an electron tunnels from one site to the next. As such, the reorganization energy is characteristic for the molecular structures involved in electron transport.[3,23] For electron transport in multiheme cytochromes or proteins embedding FeS clusters, typical reorganization energies amount to ≈1000 meV.[3,24] The junction conductance of our devices, however, showed a markedly lower reorganization energy (60−161 meV), which rules out the possibility that the conductance is mediated by cytochromes or analogous complexes. Instead, since the junction activation energy is close to the one of individual filaments, we suggest that the same molecular framework is likely responsible for the charge transport along the fibers and the charge injection into the same fibers.

A Model for Interfilament Charge Transport

The currently accepted structural model of conductive fibers of cable bacteria predicts a core formed by a tight bundle of conductive channels, surrounded by a 10−15 nm thick shell of insulating proteins[14,17,21] as schematically represented in Figure 1. Charge injection into a fiber would then imply tunneling over such distances, which is exponentially suppressed. Since tunneling events across more than 1.4 nm are considered to be negligible[3,4] the core−shell model needs to be improved upon. The scientific community has formulated a few hypothesis so far to solve this discrepancy, but no clear evidence is reported in the literature.

On one hand, it is possible that during the contacting procedure of fiber skeletons in the lab the insulating shell is mechanically thinned or removed, e.g., by scratching against gold contacts. Yet, the junctions presented in this work consist just of two overlapping fiber skeletons (or native cable bacteria), and therefore the soft interface should prevent any mechanical damage. On the other hand, charge relay centers like FeS clusters or cytochromes might be present in the insulating shell, mediating charge injection. However, Raman spectroscopy revealed that the fiber network does not contain such molecules[9,14,16] and our measurements confirm this result. Instead they suggest that the same molecular structure responsible for longitudinal charge transport is also involved in the charge injection process. Within the core−shell model for the conductive fibers of cable bacteria, this would imply that cofactors similar to those composing the conductive channels are embedded in the insulating shell and are involved in the charge injection.

We propose an alternative model that would explain our results and be qualitatively compatible with the experiments that led to the formulation of the core−shell model.[14,25] Instead of being confined to the central region of the fiber, conductive channels form a loose braid dispersed in an insulating protein matrix. We thus name this model "wire-bundle-in-matrix". The channels are mainly concentrated in the core of the fiber, but can locally reach its outer part, as displayed in Figure 5. When two of these channels are close to each other, charge hopping can occur without mediation of relay centers. This can happen between channels of the same fiber, but more remarkably also between channels of different overlapping fibers. While the likelihood of having a single favorable junction point between two channels is low, we point out that the junction area between two fiber skeletons is large (about 2 × 2 μm^2). Indeed, such variability in the local contacting between filaments could explain the wide range of junction resistances measured in this work.

https://doi.org/10.1021/acsami.6c01506
ACS Appl. Mater. Interfaces 2026, 18, 25038−25043

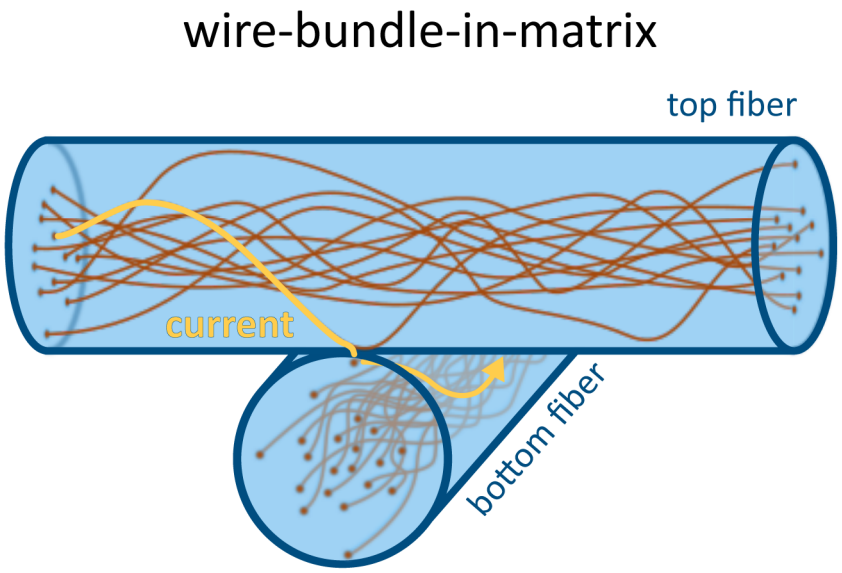

Figure 5. Schematic of charge transfer from one conductive fiber to another, assuming the "wire-bundle-in-matrix" model proposed in this work. The yellow arrow represents the current path from one fiber to the other. In this model, charge transfer from fiber to fiber can be facilitated by spatial proximity of two channels close to the surface of the fiber.

CONCLUSIONS

To summarize, we investigated the charge injection mechanism into the conductive fibers of cable bacteria. We realized junctions between fibers of different filaments by placing two filaments one on top of the other in a "cross" shape. We detected cross-fiber conduction in samples realized from fiber skeletons, but not in the ones based on native filaments. By measuring both the single-cable and the cross-cable transport, we extracted the junction resistance, and studied its dependence as a function of temperature. The junctions exhibited Arrhenius behavior, with a similar low activation energy as the one of single cables. From this we conclude that no cytochrome-like cofactor is supporting charge injection in cable bacteria. Our results suggest instead that the same molecular structure that enables transport in the fibers is also involved in the charge injection. We therefore challenge the core−shell model for the periplasmic fibers of cable bacteria, proposing instead a "wire-bundle-in-matrix" model, where direct contact to the conductive channels is possible. Recent cryo- transmission electron microscope studies[18] have shed new light on the internal structure of the fibers and support our proposed model. We foresee that further investigation of the conducting network formed by the channels will be of crucial importance for an accurate description of the conduction mechanism in cable bacteria. Such studies would benefit from improved chemical/enzymatic extraction procedures that may remove additional matrix material and loosen the conductive bundle trapped inside.

ASSOCIATED CONTENT

Supporting Information

The Supporting Information is available free of charge at https://pubs.acs.org/doi/10.1021/acsami.6c01506.

Additional materials and methods, supplementary plots and data for samples mentioned (PDF)

AUTHOR INFORMATION

Corresponding Authors

Cosimo Tommasi − *Department of Quantum Nanoscience, Kavli Institute of Nanoscience, Delft University of Technology, Delft 2628 CJ, Netherlands;* orcid.org/0000-0003-3487-6804; Email: c.tommasi@tudelft.nl

Herre S. J. van der Zant − *Department of Quantum Nanoscience, Kavli Institute of Nanoscience, Delft University of Technology, Delft 2628 CJ, Netherlands;* orcid.org/0000-0002-5385-0282; Email: h.s.j.vanderzant@tudelft.nl

Authors

Anastasia Gerzhik − *Institute of Biological Information Processing, Bioelectronics (IBI-3), Forschungszentrum Jülich, Jülich 52428, Germany; Faculty I, RWTH Aachen University, Aachen 52062, Germany*

Sebastian Heinzmann − *Department of Quantum Nanoscience, Kavli Institute of Nanoscience, Delft University of Technology, Delft 2628 CJ, Netherlands*

Silvia Hidalgo Martinez − *Department of Biology, University of Antwerp, Antwerpen 2610, Belgium*

Dirk Mayer − *Institute of Biological Information Processing, Bioelectronics (IBI-3), Forschungszentrum Jülich, Jülich 52428, Germany;* orcid.org/0000-0003-1296-8265

Filip. J. R. Meysman − *Department of Biology, University of Antwerp, Antwerpen 2610, Belgium; Department of Biotechnology, Delft University of Technology, Delft 2629 HZ, Netherlands;* orcid.org/0000-0001-5334-7655

Complete contact information is available at: https://pubs.acs.org/10.1021/acsami.6c01506

Notes

The authors declare no competing financial interest.

ACKNOWLEDGMENTS

All authors received support from the European Innovation Council Pathfinder project PRINGLE, grant 101046719. S.H.M. and F.J.R.M. received additional support from the

Research Foundation Flanders (Fonds Wetenschappelijk Onderzoek), through grants S004523N and G0ADR25N. The authors thank Dr. Jeanine Geelhoed (UAntwerpen) for developing and supplying clonal cultures of cable bacteria, and Tzu-Ping Lin (FZJ) for her support with the experimental measurements.

REFERENCES

(1) Malkin, S. Y.; Meysman, F. J. R. Rapid Redox Signal Transmission by "Cable Bacteria" beneath a Photosynthetic Biofilm. *Appl. Environ. Microbiol.* **2015**, *81*, 948−956.
(2) Meysman, F. J. R. Cable Bacteria Take a New Breath Using Long-Distance Electricity. *Trends Microbiol.* **2018**, *26*, 411−422.
(3) Moser, C. C.; Keske, J. M.; Warncke, K.; Farid, R. S.; Dutton, P. L. Nature of biological electron transfer. *Nature* **1992**, *355*, 796−802.
(4) Page, C. C.; Moser, C. C.; Chen, X.; Dutton, P. L. Natural engineering principles of electron tunnelling in biological oxidation-reduction. *Nature* **1999**, *402*, 47−52.
(5) Gray, H. B.; Winkler, J. R. Electron flow through metalloproteins. *Biochim. Biophys. Acta, Bioenerg.* **2010**, *1797*, 1563−1572.
(6) Reguera, G.; McCarthy, K. D.; Mehta, T.; Nicoll, J. S.; Tuominen, M. T.; Lovley, D. R. Extracellular electron transfer via microbial nanowires. *Nature* **2005**, *435*, 1098−1101.
(7) Xu, S.; Barrozo, A.; Tender, L. M.; Krylov, A. I.; El-Naggar, M. Y. Multiheme Cytochrome Mediated Redox Conduction through Shewanella oneidensis MR-1 Cells. *J. Am. Chem. Soc.* **2018**, *140*, 10085−10089.
(8) Bjerg, J. T.; Boschker, H. T. S.; Larsen, S.; Berry, D.; Schmid, M.; Millo, D.; Tataru, P.; Meysman, F. J. R.; Wagner, M.; Nielsen, L. P.; Schramm, A. Long-distance electron transport in individual, living cable bacteria. *Proc. Natl. Acad. Sci. U. S. A.* **2018**, *115*, 5786−5791.
(9) Meysman, F. J. R.; et al. A highly conductive fibre network enables centimetre-scale electron transport in multicellular cable bacteria. *Nat. Commun.* **2019**, *10*, 4120.
(10) Bonné, R.; Hou, J.-L.; Hustings, J.; Wouters, K.; Meert, M.; Hidalgo-Martinez, S.; Cornelissen, R.; Morini, F.; Thijs, S.; Vangronsveld, J.; Valcke, R.; Cleuren, B.; Meysman, F. J. R.; Manca, J. V. Intrinsic electrical properties of cable bacteria reveal an Arrhenius temperature dependence. *Sci. Rep.* **2020**, *10*, 19798.
(11) Pankratov, D.; Martinez, S. H.; Karman, C.; Gerzhik, A.; Gomila, G.; Trashin, S.; Boschker, H. T. S.; Geelhoed, J. S.; Mayer, D.; De Wael, K.; et al. The organo-metal-like nature of long-range conduction in cable bacteria. *Bioelectrochemistry* **2024**, *157*, 108675.
(12) Van der Veen, J. R.; Hidalgo Martinez, S.; Wieland, A.; De Pellegrin, M.; Verweij, R.; Blanter, Y. M.; van der Zant, H. S. J.; Meysman, F. J. R. Temperature-Dependent Characterization of Long-Range Conduction in Conductive Protein Fibers of Cable Bacteria. *ACS Nano* **2024**, *18*, 32878−32889.
(13) Schwarze, M.; et al. Molecular parameters responsible for thermally activated transport in doped organic semiconductors. *Nat. Mater.* **2019**, *18*, 242−248.
(14) Boschker, H. T. S.; et al. Efficient long-range conduction in cable bacteria through nickel protein wires. *Nat. Commun.* **2021**, *12*, 3996.
(15) Veen, J. R. V. D.; Valianti, S.; Zant, H. S. J. V. D.; Blanter, Y. M.; Meysman, F. J. R. A model analysis of centimeter-long electron transport in cable bacteria. *Phys. Chem. Chem. Phys.* **2024**, *26*, 3139−3151.
(16) Smets, B.; Boschker, H. T. S.; Wetherington, M. T.; Lelong, G.; Hidalgo-Martinez, S.; Polerecky, L.; Nuyts, G.; De Wael, K.; Meysman, F. J. R. Multi-wavelength Raman microscopy of nickel-based electron transport in cable bacteria. *Front Microbiol.* **2024**, *15*, 15.
(17) Digel, L.; et al. Comparison of cable bacteria genera reveals details of their conduction machinery. *EMBO Rep.* **2025**, *26*, 1749−1767.
(18) Meysman, F. J.; Smets, B.; Martinez, S. H.; Claes, N.; Schroeder, B.C.; Geelhoed, J. S.; Liu, Y.; Choyikutty, J.A.; Chennit, T.; Bodson, T. et al.A hierarchical nickel organic framework confers high conductivity over long distances in cable bacteria. *bioRxiv*, **2025**, .
(19) Cornelissen, R.; et al. The Cell Envelope Structure of Cable Bacteria. *Front. Microbiol.* **2018**, *9*, 9.
(20) Jiang, Z.; Zhang, S.; Klausen, L. H.; Song, J.; Li, Q.; Wang, Z.; Stokke, B. T.; Huang, Y.; Besenbacher, F.; Nielsen, L. P.; Dong, M. In vitro single-cell dissection revealing the interior structure of cable bacteria. *Proc. Natl. Acad. Sci. U. S. A.* **2018**, *115*, 8517−8522.
(21) Thiruvallur Eachambadi, R.; Boschker, H. T. S.; Franquet, A.; Spampinato, V.; Hidalgo-Martinez, S.; Valcke, R.; Meysman, F. J. R.; Manca, J. V. Enhanced Laterally Resolved ToF-SIMS and AFM Imaging of the Electrically Conductive Structures in Cable Bacteria. *Anal. Chem.* **2021**, *93*, 7226−7234.
(22) Gerzhik, A.; Pankratov, D.; Martinez, S. H.; Meysman, F. J. R.; Offenhäusser, A.; Mayer, D. Pullulan Coating Preserves High Conductivity in Cable Bacteria Wires. *ACS Appl. Bio Mater.* **2026**, *9*, 2591−2601.
(23) Marcus, R. A. Electron transfer reactions in chemistry theory and experiment. *J. Electroanal. Chem.* **1997**, *438*, 251−259.
(24) Tipmanee, V.; Oberhofer, H.; Park, M.; Kim, K. S.; Blumberger, J. Prediction of reorganization free energies for biological electron transfer: a comparative study of Ru-modified cytochromes and a 4-helix bundle protein. *J. Am. Chem. Soc.* **2010**, *132*, 17032−17040.
(25) Eachambadi, R. T.; Bonné, R.; Cornelissen, R.; Hidalgo-Martinez, S.; Vangronsveld, J.; Meysman, F. J. R.; Valcke, R.; Cleuren, B.; Manca, J. V. An Ordered and Fail-Safe Electrical Network in Cable Bacteria. *Adv. Biosyst.* **2020**, *4*, 2000006.

https://doi.org/10.1021/acsami.6c01506
ACS Appl. Mater. Interfaces 2026, 18, 25038−25043